Film Bulk Acoustic Wave Resonator (FBAR) Filter for Ku-band Transceiver

N. Izza M. Nor[*,**], K. Shah[*], J. Singh[*] and Z. Sauli[**]

[*]Centre for Technology Infusion, La Trobe University, 3086, Bundoora, Australia,
nimohdnor@students.latrobe.edu.au, k.shah@latrobe.edu.au, jack.singh@latrobe.edu.au
[**]School of Microelectronic Engineering, Universiti Malaysia Perlis, Malaysia,
zaliman@unimap.edu.my

ABSTRACT

This paper presents the optimisation and analysis of the Ku-band FBAR using 3-D finite element modelling (FEM) is presented. The estimation of material damping coefficients (α and β) using the Akhieser approximation is carried out to estimate more accurate values of the coefficients, thus a more realistic value of Q factor will be achieved. The value of β calculated is $3.84e^{-14}$ and the Q factor of 300-330 has been achieved for the Ku-band FBAR. The Ku-band FBAR is designed with the optimum thickness ratio of electrode to the piezoelectric material (t_m/t_p) to achieve a maximum value of the electromechanical coupling coefficient (k^2_{eff}). A maximum value of k^2_{eff} of 6.47% for series FBAR and 6.51% for shunt FBAR is achieved. This work also presents the design of Ku-band FBAR filter implemented with the optimised Ku-band FBAR by using the ABCD matrix method. The designed Ku-band FBAR filter has the centre frequency of 15.5 GHz, the insertion loss of -3.36dB, out-of-band rejection of -11.90dB and fractional bandwidth of 7.0%.

Keywords: ladder-type FBAR filter, FBAR, Ku-band filter, MEMS, AlN.

1 INTRODUCTION

As the wireless communication data and video grows, the demand for more channels and wider bandwidths are increasing. The conventional frequency bands, which are below 6 GHz are already congested, thus the need for transceiver systems working at frequencies higher than 10GHz are growing in particular in Ku-band, ranges from 12GHz to 18GHz. Cost, area and power consumption are the key figures of merit for the transceiver, however, literature highlights most of these transceivers are relatively large and heavy due to use of discrete component including filters. Various Ku-band filters are reported in literature using different designs and manufacturing methods such as defect ground structure (DGS), inter-digital structure and couple strip line filters [1-2]. However, improvement in filter performance and better integration methods with microwave monolithic integrated circuit (MMIC) and radio frequency Micro electro-mechanical systems (MEMS) technology is needed to improve integration and reduce power consumption. Film bulk acoustic wave resonator (FBAR) filter and FBAR diplexer have been developed for WiFi and WiMAX applications. These components have shown better performance and higher integration level. FBAR filters have very high quality (Q) factor, good power handling and small size. Furthermore, FBAR is compatible with MMIC and MEMS technology. FBAR filters have been reported operating in the frequency range of X-band, K-band and Ka-band [3-5]. Aluminium nitride (AlN) is a preferred piezoelectric material due to its moderate mechanical coupling factor; higher acoustic velocity and higher Q value [6] at operating frequencies higher than 10GHz compared to zinc oxide (ZnO). Material such as aluminium (Al), Platinum (Pt), Molybdenum (Mo) and ruthenium (Ru) are widely used as the electrode of the FBAR. Ru is used as the electrode material for FBAR in K-band frequency due to its higher acoustic impedance than other electrode materials [5]. The k^2_{eff} and Q factor of FBAR resonator determines the bandwidth and the efficiency of energy conversion from electrical to mechanical energy in an FBAR filter respectively [7-8]. Lower value of k^2_{eff} leads to a high insertion loss and higher value of Q leads to lower insertion loss [8]. To reduce cost, area and power consumption of Ku- band transceivers, this research aims to design, analyse and implement Ku-band filters with centre frequency of 15.5GHz and 1GHz bandwidth using FBAR.

This paper is organised as follows: Section 2 presents the design of Ku-band FBAR. Section 3 discusses the design of Ku-band FBAR filter. Section 4 presents the results and discussion. Section 5 concludes the paper.

2 DESIGN OF KU-BAND FBAR

In this work, the air-gap FBAR as shown in Fig. 1 (a) and the cross-section view of the FBAR is depicted in Fig. 2 (b) is adopted. The FBAR is designed using AlN as the piezoelectric material, Ru as the top and bottom electrodes and silicon nitride (Si_3N_4) as the membrane on silicon (Si) substrate.

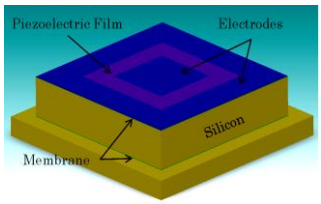

Figure 1 (a): 3-D Model

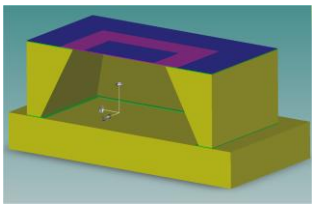

Figure 1 (b): Cross-section

Based on the parameters of the FBAR obtained from previous work in [9], the 3-D FEM is used to model the FBAR in order to obtain more realistic results. Width (W), length (L) and thickness (t) of each piezoelectric and electrode layer are varied to analyze the performance of the FBAR under different conditions. Previous studies have shown that the resonance frequency of an FBAR is determined by the thickness of the piezoelectric film where a thicker piezoelectric film results in lower resonance frequency. Therefore, in this work, the effects of other design parameters on the characteristics of FBAR are carried out as follows:

1) Influence of Electrode Materials

In this analysis, Mo and Ru are used as the electrode materials for comparison due to their excellent material properties. The thickness of Mo and Ru are varied from 5nm to 100nm while the thickness of AlN stays constant at 205nm. In this analysis, it can be seen that Mo shows the higher series resonance frequency (f_s) compared to Ru. This is due to the lower mass density of Mo and its lessened mass loading effect when compared to Ru. The mass density of Mo is 10300kg/m^3 and it is 12500kg/m^3 for Ru. It is also observed that the f_s for both electrode materials increases when the electrode thickness is reduced. Hence, it can be concluded that even though Ru has a higher acoustic velocity (6931m/s) than Mo (6213m/s), the mass loading effect is only influenced by the mass density of the material.

2) Influence of Varying Either Top or Bottom Electrode

In this analysis, the thickness of the AlN is set to 185nm, the top electrode is set constant at 25nm and the bottom electrode varies from 25nm to 45nm. On the other hand, the thickness of the AlN is set to 185nm, the bottom electrode is constant at 25nm while the top electrode varies from 25m to 45nm. In both analyses, it is observed that the f_s increases as the thickness of the variable thickness electrode decreased. Both analyses show the same f_s of the equivalent electrode thickness. Hence, the mass loading can be done either on the top or on the bottom electrode to achieve the desired resonance frequency. It is also observed that the k^2_{eff} decreases as the thickness of the electrode increases.

3) Influence of Thickness Ratio of Electrodes to Piezoelectric Film

The k^2_{eff} is a measure of the relative frequency spacing between f_s and f_p, and determines the bandwidth of a filter. According to [10] and [11], the use of a high-acoustic impedance electrode material of an FBAR is effective to achieve wideband filter and provides excellent enhancement. For this analysis, Ru and Mo are used for comparison. It is demonstrated in the analysis that the maximum k^2_{eff} achieved is 7.24% and 7.17% when the t_m/t_p is 0.1 for Ru and Mo respectively. The analysis also shows that Ru affords wider bandwidth compared to Mo. This is due to the higher acoustic impedance of Ru compared to Mo.

4) Influence of Material Damping

For the purpose of analysis, FBAR with the AlN thickness of 185nm and Ru thickness of 25nm is selected. The losses from thermoelastic damping and material damping are considered and their effect on the electrical impedance and Q factor of the FBAR is analysed. It is observed when the material damping is included, the spurious modes in the electrical impedance are suppressed. This is because material damping has damped out the harmonics. However, the Q factor of the FBAR decreases. It is further observed that the damping causes a negligible change to the f_s and parallel frequency (f_p) and the k^2_{eff} is almost constant for both FBARs.

5) Influence of Resonance Area

In this analysis, five different areas are set from 28x28μm^2 to 36x36μm^2 with constant thicknesses of AlN and Ru. The analysis shows that the area size has no significant effect on f_s, f_p, k^2_{eff} and Q factor of the FBAR. Further, it is found that area size influences the C_0 of the Ku-band FBAR, which C_0 is related to impedance matching. Area size is a critical parameter in designing the FBAR filter, thus optimisation is crucial.

3 DESIGN OF KU-BAND FBAR FILTER

There are several topologies of FBAR filters including ladder-type, lattice-type or the combination of both [12]. In this work, the ladder-type topology is chosen due to excellent performance and less number of resonators are required. Furthermore, the interconnect technique that is straightforward and easy to implement. The ladder-type FBAR filter is modelled by the nth order interconnection of series and shunt connected FBARs as depicted in Fig. 2. The total number of resonators matches the order (N) of the filter. The ladder-type filter gives a steep roll-off but a poor out-of-band (OoB) rejection characteristic. A better OoB can be achieved by cascading more L-section of the filter; however, this will trade-off with the insertion loss (I_L).

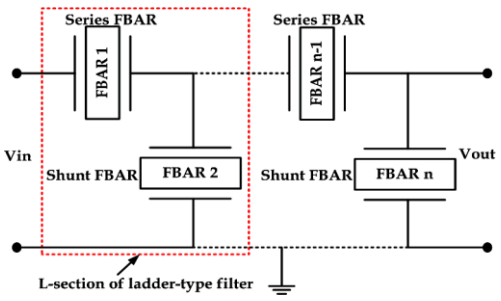

Figure 2: nth order of ladder-type FBAR filter

In this work, the FBAR filter is modelled by the transmission ABCD matrix method. A ladder-type FBAR

filter can be described by 2x2 transmission or transmission *ABCD* matrix for each two-port network within the filter. The chain matrixes of a series FBAR and shunt FBAR are given in [13-14] as follows:

$$M_s = \begin{bmatrix} 1 & Z_1 \\ 0 & 1 \end{bmatrix} \quad \text{and} \quad M_p = \begin{bmatrix} 1 & 0 \\ Y_2 & 1 \end{bmatrix} \tag{1}$$

M_s and M_p are ABCD matrices of the series and shunt FBAR respectively. Z_1 is the electrical impedance of series FBAR and Y_2 is the admittance of shunt FBAR, where Y_2 is the inverse of the impedance $Y_2=1/Z_2$. The ABCD matrix of the cascade connection of two or more two-port networks can be easily obtained by multiplying the ABCD matrices of the individual two-port network as shown below:

$$M = \begin{bmatrix} A & B \\ C & D \end{bmatrix} = M_s \cdot M_p \cdot M_s \cdots \tag{3}$$

The S_{21}-parameter of the FBAR filter is given as:

$$S_{21} = \frac{2}{A + B/Z_0 + CZ_0 + D} \tag{4}$$

where Z_0 is the source impedance (50Ω). By using the series electrical impedance (Z_s) and parallel electrical impedance (Z_p) obtained from the 3-D FEM analysis, the ABCD matrix method is used to design the filter.

4 RESULTS AND DISCUSSION

The performance of the Ku-band FBAR is improved by optimising the geometrical parameters such as the t_m/t_p and the size of the area to meet the requirement for the Ku-band FBAR filter. A higher k^2_{eff} will result in wider bandwidth while a higher Q factor will result in FBAR with better performance. Table and Table show the results of the optimised Ku-band FBAR. It has been shown that an optimum t_m/t_p will result in the highest k^2_{eff} up to 6.51%. However, in terms of the bandwidths, k^2_{eff} has no significant influence as the values of t_m/t_p of the FBAR are close to each other, which is from 0.10 to 0.15 in this research. Therefore, it showed a slight difference on the bandwidths of the FBAR. Similarly, the f_s and f_p of the FBARs are close to each other.

AlN (nm)	Ru (nm)	t_m/t_p	f_s (GHz)	f_p (GHz)	k^2_{eff} (%)	BW (GHz)	Q_s	Q_p
(1) 205	21	0.10	15.89	16.32	6.47	0.43	263	284
(2) 185	25	0.14	15.87	16.29	6.36	0.42	265	287

Table 1: Optimised series FBAR parameters

AlN (nm)	Ru (nm)	t_m/t_p	f_s (GHz)	f_p (GHz)	k^2_{eff} (%)	BW (GHz)	Q_s	Q_p
(1) 209	25	0.12	14.72	15.12	6.49	0.4	285	304
(2) 205	26	0.13	14.67	15.12	6.51	0.4	286	306

Table 2: Optimised parallel (shunt) FBAR parameters

The series FBAR (1) and shunt FBAR (2) are selected to construct the filter due to their high k^2_{eff}. The area of the series FBAR and shunt FBAR are $1.48\text{x}10^{-3}$μm^2 and $1.32\text{x}10^{-4}$ μm^2 respectively. Fig. 3 shows the electrical impedance of the FBARs. The designed Ku-band FBAR filters utilising these FBARs are depicted in Fig. 4.

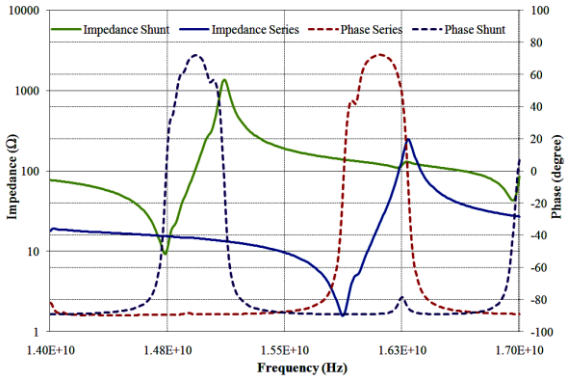

Figure 3: Electrical impedance of FBARs

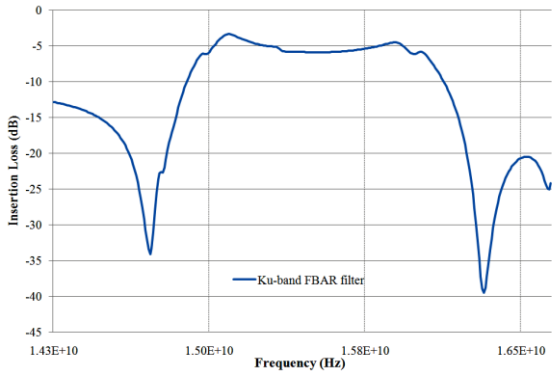

Figure 4: 8th order transmission response of FBAR filter

Table 3 shows a comparison of FBAR filters operating in X-band to Ka band. All these filters were designed with 4-stage ladder filter, which is equal to 8th order filter. The FBAR filters presented in this thesis have shown superior performance to those reported in [5], where the insertion loss is too high and the bandwidth is only 2%. To date, the FBAR filter designed in this thesis is the first FBAR filter operating in Ku-band frequency range ever reported.

Table 4 shows a comparison of Ku-band FBAR filters designed in this work with other filters operating in Ku-band. All these filters were designed using different

technology including DGS, interdigital and couple striplines.The comparison shows that the FBAR filter presented in this work has comparable performance to these other filters. Return loss of -10.55 dB is an acceptable value in filter application. However, the Ku-band FBAR filter designed in this work has the advantage of smaller area size and thus the size of the Ku-band transceiver can be reduced.

Reference	f_c (GHz)	I_L (dB)	*OoB* (GHz)	*BW* (GHz)	*N*
[3]	29.2	-3.80	-11.0	0.99	8^{th}
	23.8	-3.80	-13.0	0.81	8^{th}
[4]	19.8	-4.10	-18.0	0.39	8^{th}
[5]	9.08	-1.70	-21.0	0.28	8^{th}
This work	15.5	-3.36	-11.9	1.09	8^{th}

Table 3: Comparison of FBAR filters characteristics

Reference	[2]	[2]	[1]	This work
Filter Design	DGS	Interdigital	Couple striplines	Ladder-type FBAR
f_c **(GHz)**	14.7	15.5	14.527	15.5
I_L **(dB)**	-2.0	-1.5	-3.27	-3.36
R_L **(dB)**	-20	-15	-29.61	-10.55
***OoB* (dB)**	--	--	--	-11.90
***BW* GHz)**	0.50	1.20	1.10	1.09
Size (mm^2)	--	--	5.5x3.8	0.58x0.15
N	2^{nd}	--	--	8^{th}

Table 4: Comparison of Ku-band filter characteristics

5 CONCLUSION

The Ku-band FBAR has been designed with the optimum thickness ratio of electrode to the piezoelectric material to achieve a maximum value of k^2_{eff} of 6.47% for series FBAR and 6.51% for shunt FBAR. Therefore, FBAR with more than 1GHz bandwidth has been determined. The designed Ku-band FBARs have Q_s of 263.26 and Q_p of 284.29 for series FBAR, and k^2_{eff} of 6.51%, Q_s of 286.84 and Q_p of 306.51 for shunt FBAR. The designed Ku-band FBAR filter using the optimised FBAR has the centre frequency of 15.5 GHz, the insertion loss of -3.36dB, out-of-band rejection of -11.90dB and bandwidth of 1.09GHz. The optimised FBAR filter shows better performance and smaller size when compared with the other FBAR filters and Ku-band filters in literatures [1-5]. Therefore, the designed Ku-band FBAR filter is a suitable candidate to be implemented on the Ku-band transceiver.

REFERENCES

[1] J. Jianhua, L. Yinqiao, H. Sha, *et al.*, "A compact LTCC Transmit Receive Module at Ku-band," *International Conference on Microwave and Millimeter Wave Technology*, pp. 1239-1241, 2010.

[2] H. Su, M. Xing, Y. Li, *et al.*, "Design of a Front-end of a Ku-band Transceiver Based on LTCC Technology," *11th International Conference on Electronic Packaging Technology & High Density Packaging*, pp. 851-855, 2010.

[3] M. Hara, T. Yokoyama, T. Sakashita, *et al.*, "A Study of The Thin Film Bulk Acoustic Resonator Filters in Several Ten GHz Band," *IEEE International Ultrasonics Symposium*, pp. 851-854, 2009.

[4] M. Hara, T. Yokoyama, M. Ueda, *et al.*, "X-Band Filters Utilizing AlN Thin Film Bulk Acoustic Resonators," *IEEE Ultrasonics Symposium*, pp. 1152-1155, 2007.

[5] T. Yokoyama, M. Hara, M. Ueda, *et al.*, "K-band ladder filters employing air-gap type thin film bulk acoustic resonators," *IEEE Ultrasonics Symposium*, pp. 598-601, 2008.

[6] K.-W. Kim, G.-Y. Kim, J.-G. Yook, *et al.*, "Air-Gap Type TFBAR-based Filter Topologies," *Microwave and Optical Technology Letters*, vol. 34, pp. 386-387, 2002.

[7] Q. Chen and Q.-M. Wang, "The effective electromechanical coupling coefficient of piezoelectric thin-film resonators," *Applied Physics Letters*, vol. 86, pp. 022904-022904-3, 2005.

[8] G. F. Perez-Sanchez and A. Morales-Acevedo, "Design of bulk acoustic wave resonators based on ZnO for filter applications," *6th International Conference on Electrical Engineering, Computing Science and Automatic Control*, pp. 1-6, 2009.

[9] K. S. N.Izza M.Nor, J.Singh and Z.Sauli, "Design and Simulation of Film Bulk Acoustic Wave Resonator in Ku-band," *Advanced Materials Research*, vol. 662, pp. 556-561, 2013.

[10] K. M. Lakin, J. Belsick, J. F. McDonald, *et al.*, "Improved bulk wave resonator coupling coefficient for wide bandwidth filters," *IEEE Ultrasonics Symposium*, pp. 827-831 vol.1, 2001.

[11] T. N. M. Ueda, S. Taniguchi, T. Yokoyama, J. Tsutsumi, M. Iwaki, and Y. Satoh, "Film Bulk Acoustic Resonator using High-Acoustic-Impedance Electrodes," *Jpn. J. Appl. Phys.*, vol. 46, pp. 4642-4646, 2007.

[12] A. A. Shirakawa, J.-M. Pham, P. Jarry, *et al.*, "Design of FBAR filters at high frequency bands," *International Journal of RF and Microwave Computer-Aided Engineering*, vol. 17, pp. 115-122, 2007.

[13] D. M. Pozar, "Microwave Network Analysis," *Microwave Engineering*, 2nd ed New York: John Wiley & Sons, 1988, pp. 206-237.

[14] Q. X. Su, P. Kirby, E. Komuro, *et al.*, "Thin-Film Bulk Acoustic Resonators and Filters Using ZnO and Lead-Zirconium-Titanate Thin Films," *IEEE Transactions on Microwave Theory and Techniques* vol. 49, pp. 769-778, 2001.